Constraining new physics with searches for long-lived particles: Implementation into SModelS *[Constraining new physics with searches for long-lived particles WITH SModelS]*?

Jan Heisig

Institute for Theoretical Particle Physics and Cosmology, RWTH Aachen University, 52056 Aachen, Germany

Andre Lessa

Centro de Ciências Naturais e Humanas, Universidade Federal do ABC, Santo André, 09210-580 SP, Brazil

Sabine, Wolfgang,...?

Abstract

Long-lived particles have received an increasingly attention from both the experimental and theoretical communities, due to their possible connection to Dark Matter and novel collider signatures. In this letter we discuss how some of the collider results for long-lived particles re-interpreted within simplified models can be a powerful tool for constraining interesting models. For this purpose we present an implementation of (lepton-like) heavy stable charge particle (HSCP) and R-hadron signatures into SModelS 1.2, including searches performed at the 8 and 13 TeV LHC. Using the (publicly available) SModelS 1.2 tool we investigate how these searches impact two physics scenarios: the Two Higgs Inert Doublet Model (IDM) and a gravitino dark matter model containing long-lived staus. While missing energy searches are not able to constrain any significant part of the cosmologically allowed parameter space of the IDM model, we find that HSCP searches are sentive up to dark matter masses of 550 GeV (for small mass splittings within the inert doublet). The gravitino dark matter model on the other hand can be constrained by both HSCP and R-hadron searches, which can become valuable for determining the allowed ranges of the cosmological reheating temperature in this scenario.

1. Introduction

Exploring physics beyond the standard model (BSM) is one of the key scientific goals of the LHC. Simplified models have turned out to provide useful benchmarks for interpreting LHC results and investigating their implications aiming to answer the open questions of today's fundamental physics. SModelS [1, 2] provides a very efficient framework for this reinterpretation by decomposing the signal of an arbitrary new physics model (respecting a Z_2 symmetry or a larger symmetry with a Z_2 subgroup) into simplified model topologies. This allows one to directly use the cross section upper limits or efficiency maps provided by the experimental collaborations within the simplified model framework to constrain a larger variety of BSM scenarios.[1]

So far SModelS assumed that all stable particles were neutral and only included BSM searches for missing transverse momentum (MET). However, it has widely been recognized that well-motivated BSM theories can provide non-neutral long-lived particles (LLPs) leading to distinct signatures, often providing great sensitivity at the LHC []. In this letter we make use of the novel features of SModelS 1.2 [7] to investigate well-motivated full BSM models containing LLPs. Besides being able to decompose models with long-lived charged particles, this version also includes a treatment of metastable particles and constraints for heavy stable charged particles (HSCPs) and R-hadrons[2] in its database. In particular, we improve upon previous work [8] adding efficiency maps for the CMS 13 TeV HSCP analysis [9] and reconsidering the modeling of intermediate life-

[1] A certain degree of approximation is included in this procedure, since it neglects properties like the exact production mechanism and the spin of the particles in decays, see Ref. [3–6] for specific discussions.

[2] For simplicity we label electrically charged and color neutral heavy stable particles as HSCPs. Long-lived colored particles, which can hadronize and form electrically charged bound states are always referred to as R-hadrons.

times. We also include the experimental cross section upper limits for the direct production of HSCPs [9, 10] and R-hadrons [9]. Finally, SModelS 1.2 is made publicly available.[3]

We make use of SModelS 1.2 to investigate how the searches for HSCPs and R-hadrons mentioned above impact two new physics scenarios. The first one, the Two Higgs Inert Doublet Model (IDM), provides one of the simplest dark matter models supplementing the Standard Model by just one additional $SU(2)$ (Higgs) doublet. While MET searches are scarcely sensitive to the cosmologically allowed region of the IDM parameter space, we show that for small mass splittings within the inert doublet a large range of dark matter masses can be tested by the HSCP searches.

Secondly, we consider the minimal supersymmetric standard model (MSSM) where the gravitino is assumed to be the lightest supersymmetric particle (LSP) and the stau to be next-to-LSP (NLSP). This is a cosmologically attractive scenario allowing to alleviate the gravitino problem *[REF?]* and to accommodate large reheating temperatures $T_{\rm R} \sim 10^9$ GeV in the early Universe while respecting bounds from big bang nucleosynthesis (BBN) []. The complexity of the model reveals a large number of contributing topologies including R-hadron signatures relevant for both squarks and gluinos when their decays are 3- or 4-body suppressed. We show that the LLP results have the potential to be competitive with cosmological constraints and impact the allowed range for the reheating temperature. *[Some more refs?]*

The remainder of this letter is structured as follows. In Sec. 2 we briefly review the implementation of LLP signatures into SModelS. The impact for the IDM and gravitino scenarios is presented in Sec. 3. We conclude in Sec. 4. Finally, in Appendix A and Appendix B we provide details about the recasting of the HSCP analyses and a discussion about the treatment of intermediate lifetimes, respectively.

2. Implementation in SModelS

Given the particle width, branching ratios (BRs) and total production cross-sections of a certain BSM model, SModelS performs a decomposition of the input model into a coherent sum of simplified model topologies [1, 2]. Each topology represents a pair of (prompt) cascade decays which terminate in a long-lived (BSM) particle. While previous versions assumed all particles to either have prompt decays or to be long-lived (in collider scales), version 1.2 [7] includes a calculation for the fraction of prompt decays ($\mathcal{F}_{\rm prompt}$) and decays outside the detector ($\mathcal{F}_{\rm long}$), which can be relevant for metastable particles with proper lifetimes within ∼few cm to ∼few m. [8] These fractions are used during decomposition to rescale the branching ratios, thus resulting in an effective topology cross-section ($\tilde{\sigma}$) given by:

$$\tilde{\sigma} = \sigma_{\rm prod} \left(\prod_i {\rm BR}_i \times \mathcal{F}^i_{\rm prompt} \right) \mathcal{F}^X_{\rm long} \mathcal{F}^Y_{\rm long} \,, \quad (1)$$

where $\sigma_{\rm prod}$ is the production cross section of the mother particles and X, Y are the BSM final states of the two decay chains while i runs over all intermediate BSM particles. Given the particle proper lifetime (τ), the fraction of produced particles which decay promptly ($\mathcal{F}_{\rm prompt}$) and decay outside the detector ($\mathcal{F}_{\rm prompt}$) can be approximated by:

$$\mathcal{F}_{\rm prompt} = 1 - \exp\left(-\frac{1}{c\tau} \left\langle \frac{\ell_{\rm inner}}{\gamma\beta} \right\rangle_{\rm eff} \right) \quad (2)$$

and

$$\mathcal{F}_{\rm long} = \exp\left(-\frac{1}{c\tau} \left\langle \frac{\ell_{\rm outer}}{\gamma\beta} \right\rangle_{\rm eff} \right) , \quad (3)$$

where we choose $\langle \ell_{\rm inner}/\gamma\beta \rangle_{\rm eff} = 1\,{\rm mm}$ and $\langle \ell_{\rm outer}/\gamma\beta \rangle_{\rm eff} = 7\,{\rm m}$ requiring long-lived particles to traverse the entire detector. A detailed motivation of the above expressions and values is given in Appendix B. Note that this choice is conservative, since the signature of particles decaying inside the detector may provide additional sensitivity. However, such cases introduce a dependence on the decay products of the long-lived particle which is left for future work.

All topologies terminating in long-lived neutral particles provide a signature of missing transverse energy (MET) and can be constrained by the bulk of SUSY searches. These, however, do not apply to topologies which end with a color or electrically-charged BSM final state. In order to test these scenarios SModelS 1.2 includes the CMS searches for HSCPs, color-octet (gluino-like) R-hadrons and color-triplet (squark-like) R-hadrons at 8 TeV [11] and 13 TeV [9] center-of-mass energies. For the 8 TeV HSCP results we make use of the recasting provided in Ref. [10], while a dedicated recasting was performed for the 13 TeV results (see Appendix A for details). This allowed us to compute efficiency maps for the 8 simplified model topologies introduced in Ref. [8], which are included in the SModelS 1.2 database. For the R-hadron searches we consider only the

[3] The SModelS tool and database are available at http://smodels.hephy.at

direct production topology[4] and make use of the cross section upper limits from Refs. [9, 11], which are also included in the SModelS database.

3. Physics applications

In the following we use SModelS within two BSM scenarios and derive constraints on their parameter space. We consider the inert doublet model as well as a supersymmetric scenario with a gravitino LSP and a stau NLSP.

3.1. The inert doublet model

The IDM is a two-Higgs doublet model with an exact $\mathcal{Z}_2$ symmetry, under which all standard model fields (including the Higgs doublet H) are assumed to be even, while the second scalar doublet Φ is odd. It supplements the standard model Lagrangian by the gauge kinetic terms for Φ as well as additional terms in the scalar potential, which now reads

$$\begin{aligned} V = {} & \mu_1^2|H|^2 + \mu_2^2|\Phi|^2 + \lambda_1|H|^4 + \lambda_2|\Phi|^4 \\ & + \lambda_3|H|^2|\Phi|^2 + \lambda_4|H^\dagger\Phi|^2 \\ & + \lambda_5/2\left[(H^\dagger\Phi)^2 + \text{h.c.}\right]. \end{aligned} \tag{4}$$

After electroweak symmetry breaking the model contains five physical scalar states with masses given by

$$\begin{aligned} m_{h^0}^2 &= \mu_1^2 + 3\lambda_1 v^2\,, \quad m_{H^0}^2 = \mu_2^2 + \lambda_L v^2\,, \\ m_{A^0}^2 &= \mu_2^2 + \lambda_S v^2\,, \quad m_{H^\pm}^2 = \mu_2^2 + \frac{1}{2}\lambda_3 v^2\,. \end{aligned} \tag{5}$$

where

$$\lambda_{L,S} = \frac{1}{2}\left(\lambda_3 + \lambda_4 \pm \lambda_5\right)\,, \tag{6}$$

After imposing $m_{h^0} \simeq 125.09\,\text{GeV}$ [12], we are left with five free physical parameters: m_{H^0}, m_{A^0}, $m_{H^\pm}$, λ_L and λ_2. *[not λ_S?]*

Despite its simplicity, the IDM leads to a rich phenomenology and provides a viable dark matter candidate with observable signatures in direct and indirect detection experiments. For recent accounts see *e.g.* [13–15]. At the LHC the IDM is extremely difficult to observe via MET searches [16–21]. For instance, a reinterpretation of dilepton plus MET signatures at the 8 TeV LHC [22] provides sensitivity up to $m_{H^0} \simeq 55\,\text{GeV}$ only [21]. However, in this low-mass region, the H^0 thermal relic density (Ω_{IDM}) is above the observed dark matter density (Ω_{CDM}). There are three regions where the IDM can account for the entire observed relic density ($55\,\text{GeV} \lesssim m_{H^0} \leq m_{h^0}/2$, $m_{H^0} \simeq 72\,\text{GeV}$ and $m_{H^0} \gtrsim 500\,\text{GeV}$) and a region where it can account only for a fraction of Ω_{CDM} ($72 \lesssim m_{H^0} \lesssim 500\,\text{GeV}$) [15, 23].

In this work we focus on the region with small mass splittings ($\Delta m = m_{H^\pm} - m_{H^0} \leq 1\,\text{GeV}$) and use SModelS 1.2 to reinterpret the LHC limits from HSCP searches within the IDM model. For this purpose we perform a scan over the IDM 5-dimensional parameter space restricted to:

$$\begin{aligned} 100\,\text{GeV} \leq {} & m_{H^0} & \leq 1\,\text{TeV} \\ m_{H^0} < {} & m_{A^0} & \leq 1.1\,\text{TeV} \\ 10\,\text{MeV} \leq {} & m_{H^\pm} - m_{H^0} & \leq 1\,\text{GeV} \\ -4\pi \leq {} & \lambda_L & \leq 4\pi \\ 10^{-6} \leq {} & \lambda_2 & \leq 4\pi \end{aligned} \tag{7}$$

and we impose $10^{-3} \leq R \equiv \Omega_{\text{IDM}}/\Omega_{\text{CDM}} \leq 1$. In addition we take into account constraints from Higgs invisible decays [29], electroweak precision observables [30, 31], from searches for charginos and neutralinos at LEP-II [16, 32]. indirect detection limits from γ-ray observations of dwarf spheroidal galaxies [33] and theoretical constraints on unitarity, perturbativity and vacuum stability computed with 2HDMC [31] (see Ref. [15] for further details[5]). In the following we only consider points allowed within the 2σ region of the above constraints. We use the nested-sampling algorithm MultiNest [35, 36] to efficiently explore the parameter space.

For the allowed parameter space we compute the decay tables and production cross sections with MadGraph5_aMC@NLO [37] and compute the LHC constraints with SModelS 1.2. For each parameter space point the constraining power of LHC searches can be conveniently parametrized by the ratio of the relevant signal cross-section (σ_{th}) to the corresponding analysis upper limit (σ_{UL}): $r = \sigma_{th}/\sigma_{UL}$ (see Ref. [2] for more details). If $r \geq 1$ for at least one analysis we consider the point as being excluded.

In Fig. 1 we show the impact of the LHC constraints on the IDM parameter space. In the left panel we display the signal strength r in the m_{H^0}-$c\tau_{H^\pm}$ plane while the right panel shows the dark matter fraction R in the m_{H^0}-Δm plane. Although r does in principle depend on all the model parameters, we can see that it is mostly driven by the charged Higgs mass and its lifetime. We hence show an approximate exclusion curve in the plot. As we can see, for large lifetimes,

[4] As R-hadrons are strongly produced their production via cascade decays in typically expected to be less important.

[5] With respect to Ref. [15], in this work we update direct detection constraints additionally imposing the 90% CL upper limits on the spin-independent dark matter-nucleon scattering cross section recently obtained by Xenon1T [34].

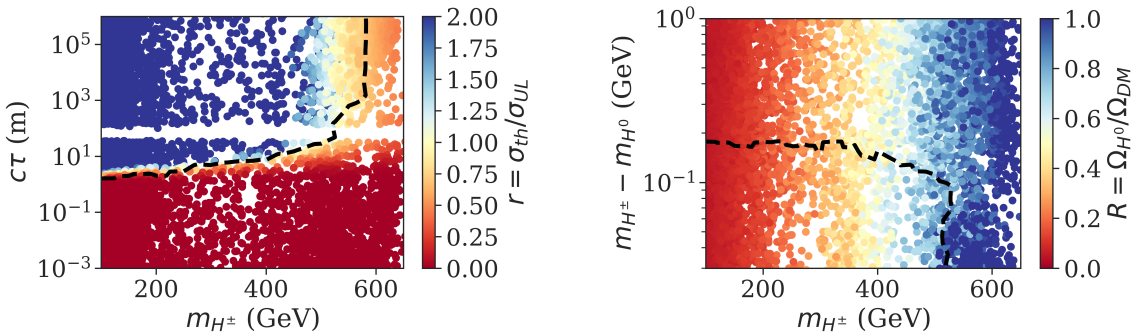

Figure 1: Allowed IDM parameter points (imposing all but the LHC constraints) in the $m_{H^\pm}$-$c\tau$ plane (left panel) and $m_{H^\pm}$-Δm (right panel). The color denotes the LHC signal strength r and the dark matter fraction R, respectively. The black dashed curve shows the (interpolated) 95% CL exclusion contour from the LHC ($r = 1$).

$c\tau \gtrsim 100\,\text{m}$, we are able to exclude points up to $m_{H^\pm} \simeq 500\,\text{GeV}$. Since we consider regions with very small mass splittings, this bound also applies to the dark matter mass, m_{H^0}. We have verified that, as expected, the HSCP searches are the single responsible by the exclusion shown.

For even smaller splittings – approaching quasi-stabile limit – the limit reaches up to around 540 GeV maximally.

This curve is also shown in the right panel.

[Needs to be put in sentences: which topologies contribute how much (reach goes above what expected from $H^\pm H^\mp$ alone); limit in $c\tau$; $c\tau$ versus Δm mapping; some words about the gap at around 100MeV; comment on exclusion versus R, that is, cosmo implications; compare to the conclusion from [14]; disappearing tracks]

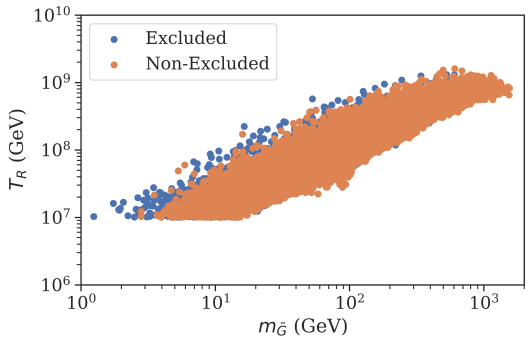

Figure 2: Effect of the LHC exclusion bounds on the otherwise allowed points in the plane spanned by the gravitino mass and reheating temperature.

3.2. Gravitino dark matter scenario

The gravitino – the superpartner of the graviton – is an attractive dark matter candidate in supersymmetric theories [38, 39]. Redering the gravitino to be the LSP can alleviate the gravitino problem which appears in neutralino LSP scenarios [40–43] unless the gravitino is much heavier than the rest of the supersymmetric spectrum which in turn severely limits the viable options for supersymmetry breaking. For a gravitino LSP the lightest sparticle of the MSSM (*i.e.* the NLSP) can be any sparticle. However, in order to not reintroduce a severe problem through late decays of the NLSP – spoiling successful BBN predictions [44] – certain choices appear more promising. For instance, the stau is an attractive NLSP candidate providing a large annihilation cross section that reduces its freeze-out abundance. On the one hand this helps to evade bounds from BBN. On the other hand it reduces the contribution to the gravitino abundance through NLSP decays. This allows for a larger thermal contribution of gravitino production while not over-closing the Universe. Since the thermal contribution is (approximately) proportional to the reheating temperature, $\Omega^{\text{th}}_{\widetilde{G}} \propto T_{\text{R}}$ [45–47], it allows for higher values of T_{R}, as preferred by classes of models for leptogenesis and inflation.

Here we revisit the parameter scan performed in [48, 49] refining and updating the constraints from long-lived particle searches at the LHC. In [48] searches for HSCPs and R-hadrons at the the 8 TeV LHC have been taken into account. The respective constraints from HSCP have been computed in an approximate way using the efficiencies from the direct production channel and the gaugino mediated supersymmetry breaking model as representative benchmarks.

The scan is performed in the framework of the pMSSM. Imposing the additional assumption $m_{\tilde{q}_{1,2}} \equiv m_{\widetilde{Q}_{1,2}} = m_{\tilde{u}_{1,2}} = m_{\tilde{d}_{1,2}}$ we achieve a 17-dimensional parameter space with input parame-

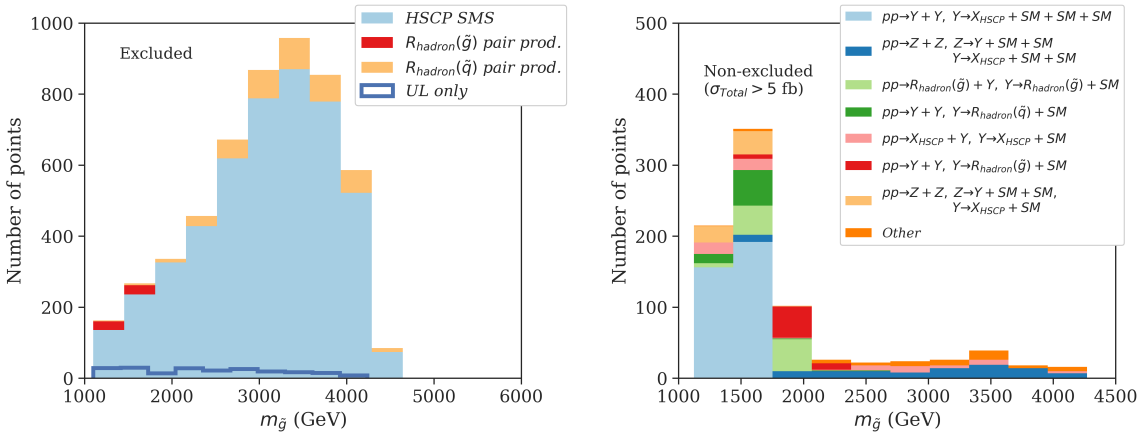

Figure 3: Left panel: Number of excluded points as a function of the gluino mass. The color indicates the channel which leads to the exclusion. *[more precisely?]* The blue line indicates the number of points excluded by HSCP upper cross section limits only. Right panel: Number of non-excluded points with a total SUSY production cross section of more than 5 fb. The color indicates the dominant channel among the missing topologies.

ters and scan ranges:[6]

$$\begin{aligned}
-10\,\text{TeV} \leq\ & A_t & \leq 10\,\text{TeV} \\
-8\,\text{TeV} \leq\ & A_b,\, A_\tau,\, \mu & \leq 8\,\text{TeV} \\
1 \leq\ & \tan\beta & \leq 60 \\
100\,\text{GeV} \leq\ & m_A & \leq 4\,\text{TeV} \\
200\,\text{GeV} \leq\ & m_{\tilde{\tau}_1} & \leq 2\,\text{TeV} \\
700\,\text{GeV} \leq\ & m_{\tilde{t}_1}, m_{\tilde{b}_1} & \leq 5\,\text{TeV} \\
0 <\ & \theta_{\tilde{\tau}}, \theta_{\tilde{t}} & < \pi \\
m_{\tilde{\tau}_1} \leq\ & m_{\tilde{L}_{1,2}}, m_{\tilde{e}_{1,2}} & \leq 4\,\text{TeV} \\
1.2\,\text{TeV} \leq\ & m_{\tilde{q}_{1,2}} & \leq 8\,\text{TeV} \\
m_{\tilde{\tau}_1} \leq\ & M_1, M_2 & \leq 4\,\text{TeV} \\
1\,\text{TeV} \leq\ & M_3 & \leq 5\,\text{TeV}
\end{aligned} \tag{8}$$

The particle spectrum has been computed with SuSpect 2.41 [50] and FeynHiggs 2.9.2 [51]. The following hard constraints were required. The lighter stau $\tilde{\tau}_1$ has to be the lightest sparticle within the MSSM and m_h or/and $m_H \in [123; 128]$ GeV [12, 52].

The decay widths and branching ratios have been computed with SDecay [53, 54] and (in the case of missing dominant decay channels) MadGraph5_aMC@NLO [37], while the freeze-out abundance of staus have been computed with micrOMEGAs 2.4.5 [55]. We considered constraints on the MSSM Higgs sector, performed at LEP, the Tevatron and the LHC [56] and EW precision bounds [57–59] as well as theoretical constrains arising from charge or color breaking vacua [60–65]. With respect to [48] we imposed updated constraints on flavor constraints and $\text{BR}(B \to X_s\gamma) \in [3.0; 3.64] \times 10^{-4}$ [66] and $\text{BR}(B_s^0 \to \mu^+\mu^-) \in [1.74; 4.34] \times 10^{-9}$ [67] and on the MSSM Higgs sector by applying the conservative constraints on m_A and $\tan\beta$ derived in the $m_h^{\text{mod+}}$-scenario [68].

For each point in the pMSSM parameter space 10 gravitino masses have been randomly generated. Among other conditions the respective mass range is govern by the requirement that the total gravitino abundance can match the measured dark matter abundance,

$$\Omega_{\tilde{G}}^{\text{non-th}} h^2 + \Omega_{\tilde{G}}^{\text{th}} h^2 = \Omega_{\text{CDM}} h^2\,, \tag{9}$$

where $\Omega_{\tilde{G}}^{\text{th}} h^2$ is a function of T_R [45–47] such that (9) is used to compute the respective T_R that saturates $\Omega_{\text{CDM}} h^2 = 0.1189$. For each of the resulting points in the (17+1)-dimensional parameter space (that by construction fulfills the relic density constraint) constraints from BBN [69, 70][7] have been imposed which depend on the freeze-out abundance, the lifetime and the hadronic branching ratios of the stau decaying into the gravitino. The latter have been computed with the spin-3/2 extension of MadGraph [73, 74]. For further details we refer to [48, 49].

Here we use SModelS 1.2 to decompose the signal into all occurring simplified model topologies, including and constrain them by 8TeV HSCP

[6] In this phenomenologically driven parameter scan the spectrum parameters of the third generation sfermions, $m_{\tilde{\tau}_1}$, $m_{\tilde{t}_1}$, $m_{\tilde{b}_1}$, $\theta_{\tilde{\tau}}$ and $\theta_{\tilde{t}}$, were chosen as input parameters in order to obtain an equally good coverage of small and large mixing scenarios. Tree-level relations were used to translate these parameters into soft parameters. In the further analysis only the values recalculated by the spectrum generator are used consistently.

[7] Furthermore, constraints from diffuse gamma ray observations [71, 72] have been consider, which, however, have found to be much less relevant [49].

as well as 13TeV HSCP and R-hadron searches. *[More?]* The cross sections are computed with PYTHIA 8 [] and NLLFAST [].

The result is shown in Fig. 2. *[Discuss. Missing topologies: 1. HSCP + 4-body decays (gluino -¿ sq* + jet -¿ ewino* + q -¿ f + stau. So it happend for mstau ¡ mgluino ¡ mEWinos,msquarks.]*

4. Conclusion

In this work we announced SMODELS 1.2 which is capable to test BSM models that contain non-neutral long-lived particles. We implemented HSCP and R-hadron searches at the 8 and 13 TeV LHC. We discuss to benchmark scenarios in order to illustrate its capabilities, the IDM and a gravitino dark matter scenario.

[...]

Acknowledgements

We would like to thank Nishita Desai, Suchita Kulkarni, Sabine Kraml, Wolfgang Waltenberger *[if not authors]* ,... for very helpful discussions.

This work is supported by the German Research Foundation DFG through the research unit "New physics at the LHC".

Appendix A. Recasting and validation

In this appendix we detail the recasting of the 8 and 13 TeV HSCP searches used in SMODELS. We first review the recasting for the 8 TeV CMS HSCP analysis presented in [10]. The authors of [10] provide signature efficiencies for the off- and online selection criteria, $P_{\text{on}}(\boldsymbol{k})$ and $P_{\text{off}}(\boldsymbol{k})$, respectively, as a function of the generator-level kinematics, $\boldsymbol{k} = (\eta, p_{\text{T}}, \beta)$, of isolated[8] HSCP candidates. The signal efficiency for a given parameter point can be computed from the generated events:

$$(\mathcal{A}\epsilon) = \frac{1}{N}\sum_{i=1}^{N} \mathcal{P}^i_{\text{event}} \tag{A.1}$$

where the sum runs over all N events and

$$\mathcal{P}^i_{\text{event}} = \mathcal{P}^i_{\text{on}} \times \mathcal{P}^i_{\text{off}} \tag{A.2}$$

with

$$\begin{aligned}\mathcal{P}^i_{\text{on/off}} = {} & P_{\text{on/off}}(\boldsymbol{k}^i_1) + P_{\text{on/off}}(\boldsymbol{k}^i_2) \\ & - P_{\text{on/off}}(\boldsymbol{k}^i_1) \times P_{\text{on/off}}(\boldsymbol{k}^i_2)\,.\end{aligned} \tag{A.3}$$

For one HSCP candidate in an event the formula holds with $P_{\text{on/off}}(\boldsymbol{k}^i_2) = 0$. The left panel of figure A.4 shows the comparison of the upper cross section limits from SMODELS with the ones from [10] for direct pair production of staus. The difference is below 5%, compatible with Monte Carlo errors.

For the respective 13 TeV analysis [9] such a recast has not been provided. However, the search criteria of the 8 and 13 TeV analysis are very similar. The two analyses only differ in a slightly stronger cut on the ionization loss and time-of-flight both effectively amounting to a slightly stronger cut on the velocity in the latter analysis.[9] Hence, the 8 TeV signature efficiencies may hold for the 13 TeV to some degree of approximation. Reference [75] reported an attempt to model the 13 TeV signature efficiencies by multiplying the 8 TeV ones with a velocity dependent correction function fitted in order to resemble the signal efficiencies reported in [9]. On top of the slight reduction of the signature efficiencies for high velocities this study revealed a better performance of the CMS detector in the region of low velocities leading to a larger signal efficiencies for large HSCP masses. This latter feature could, however, not be described by a universal velocity dependent correction function for direct pair production and inclusive production. It needs further insights into the changes of the detector between run 1 and run 2 that are not provided outside the collaboration. Here, we hence follow a conservative approach taking into account the reduction of the efficiency due to the slightly stronger cuts on the velocity of the HSCP candidate. We model this by multiplying $P_{\text{off}}(\boldsymbol{k})$ with a correction function that is assumed to depend only on β:

$$f^{\text{corr}}_{(a,b)}(\beta) = \left(1 + \mathrm{e}^{a(\beta - b)}\right)^{-1} \leq 1 \tag{A.4}$$

We determine the parameters a, b in a global fit to the signal efficiencies for the pair production and inclusive production model reported in [9]. To this end we define a χ^2 by

$$\chi^2 = \sum_m \frac{\left((\mathcal{A}\epsilon)^m_{(a,b)} - (\mathcal{A}\epsilon)^m_{\text{CMS}}\right)^2}{\sigma^2_{\mathcal{A}\epsilon}}\,, \tag{A.5}$$

where $(\mathcal{A}\epsilon)^m_{(a,b)}$ is the signal efficiency for a mass point m of the considered model using the signature efficiencies with the correction function $f^{\text{corr}}_{(a,b)}$ and $(\mathcal{A}\epsilon)^m_{\text{CMS}}$ is the respective signal efficiency reported in [9]. The characteristic size of

[8] Details on the imposed isolation criteria can be found in [8, 10].

[9] The effect of slightly stronger cut on p_{T} [9] is found to be negligible for masses of a few hundred GeV.

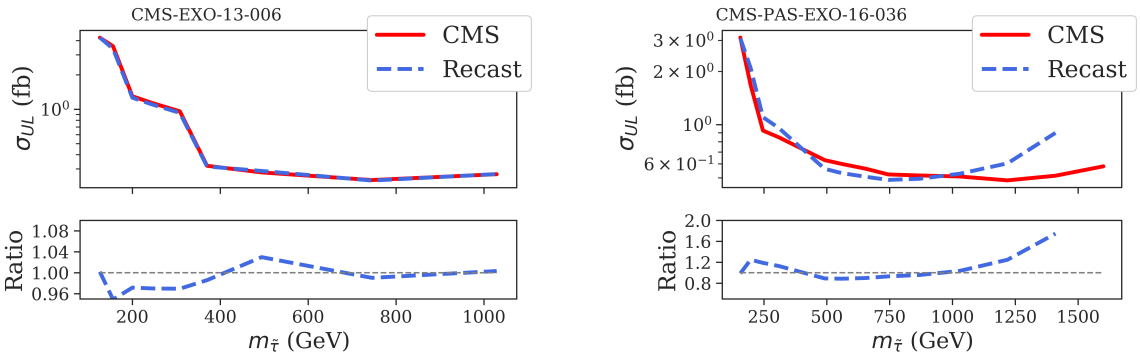

Figure A.4: Validation of the 8 TeV (left panel) and 13 TeV (right panel) CMS analysis for direct production of staus. The red and blue dashed curves show the respective cross section upper limits from CMS and from our recast.

the uncertainty, $\sigma_{\mathcal{A}\epsilon}$, is (arbitrarily) set to 0.02, which roughly reflects the precision of the recasting we aim at. We minimize the χ^2 using MULTINEST [35, 36] to explore the parameter space. The fit turns out to prefer a very sharp cut in β resembling an approximate Heaviside step function for which the value of a is not constrained beyond being larger than 150. The best-fit parameters are $a \simeq 500$, $b = 0.807$. This result was obtained by choosing all six mass points for both the direct pair production and inclusive production model. However, it is not sensitive to the exact set of model points used in the fit, in particular we get very similar results when using one or the other model only. The corresponding signal efficiencies for direct production of staus is shown in the right panel of Fig. A.4. Below a TeV the deviations are within 20% while for large HSCP masses the recasting becomes significantly conservative due to the above mentioned effects.

Appendix B. Finite lifetimes

Although the HSCP searches considered here are aimed for detector-stable particles they can also constrain models with intermediate decay length of the order of the detector size where only a certain fraction of particles decay after traversing the entire sensitive detector and hence $\mathcal{F}_{\text{long}}$ may be significantly smaller than one. In this case the resulting signal efficiency becomes very sensitive to the choice of $\langle \ell_{\text{outer}}/\gamma\beta \rangle_{\text{eff}}$. We shall therefore investigate the validity of the choice made in Sec. 2 for a representative set of different models. Our aim is to choose $\langle \ell_{\text{outer}}/\gamma\beta \rangle_{\text{eff}}$ such that the corresponding efficiencies (and hence cross section upper limits) match the ones from a full simulation in which we take into account the probabilities of a particle to decay outside the detector on an event-by-event basis using

$$F_{\text{long}}(\boldsymbol{k}) = \exp\left(-\frac{\ell_{\text{outer}}(|\eta|)}{\gamma\beta}\frac{1}{c\tau}\right). \tag{B.1}$$

Here $\gamma = (1-\beta^2)^{-1/2}$ and $\ell_{\text{outer}}(|\eta|)$ is the travel length through the CMS detector which we approximate by considering a cylindrical volume with radius of 7.4 m and length of 10.8 m.

We compute the signal efficiency with eq. (A.1) but instead of eq. (A.2) using

$$\begin{aligned}\mathcal{P}^i_{\text{event}} = {} & F_{\text{long}}(\boldsymbol{k}^i_1)P_{\text{on}}(\boldsymbol{k}^i_1)P_{\text{off}}(\boldsymbol{k}^i_1)\big(1-F_{\text{long}}(\boldsymbol{k}^i_2)\big) \\ & + F_{\text{long}}(\boldsymbol{k}^i_2)P_{\text{on}}(\boldsymbol{k}^i_2)P_{\text{off}}(\boldsymbol{k}^i_2)\big(1-F_{\text{long}}(\boldsymbol{k}^i_1)\big) \\ & + F_{\text{long}}(\boldsymbol{k}^i_1)F_{\text{long}}(\boldsymbol{k}^i_2)\mathcal{P}^i_{\text{on}}\mathcal{P}^i_{\text{off}}\,.\end{aligned} \tag{B.2}$$

Figure B.5 shows results for $\langle \ell_{\text{outer}}/\gamma\beta \rangle_{\text{eff}}$ that – using eq. (1)–(3) – yields the same efficiency as performing the full simulation using eq. (B.2). We exemplary display direct production of staus (left panel) and a 1-step decay topology (right panel). The choice $\langle \ell_{\text{outer}}/\gamma\beta \rangle_{\text{eff}} = 7\,\text{m}$ which provides (mostly) conservative results such that we do not (significantly) overestimate the signal efficiency and hence the constraining power. This can be seen looking at the corresponding 95% CL upper limits shown for the event-based computation of $\ell_{\text{outer}}/\gamma\beta$ and this approximation. *[used NLLfast for xs]*

[Maybe say at some point that in [8] $\ell_{outer}/\gamma\beta = 10/0.6\,m$ was used.]

References

[1] S. Kraml, S. Kulkarni, U. Laa, A. Lessa, W. Magerl, D. Proschofsky-Spindler, and W. Waltenberger, *SModelS: a tool for interpreting simplified-model results from the LHC and its application to supersymmetry*. Eur. Phys. J. **C74** (2014) 2868, arXiv:1312.4175 [hep-ph].

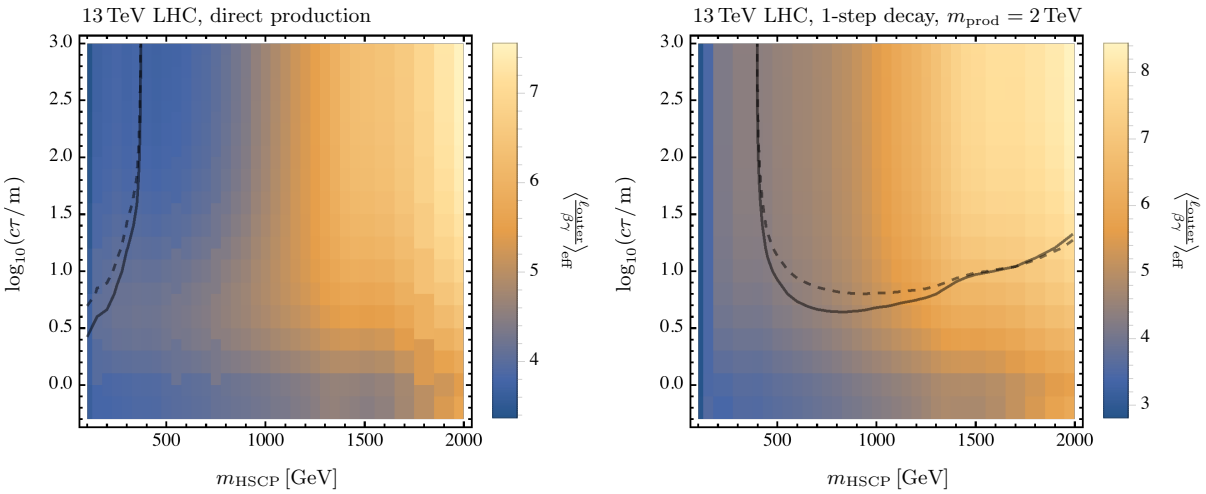

Figure B.5: The effective characteristic travel length, $\langle \ell_{\rm outer}/\gamma\beta \rangle_{\rm eff}$ (see text for details) in the parameter plane spanned by the HSCP mass, $m_{\rm HSCP}$, and its proper decay length, $c\tau$ for direct production (left panel) and for the 1-step decay topology where we choose $m_{\rm prod} = 2\,$TeV for the mass of the produced mother particle (right panel). The solid and dashed curves denote the 95% CL exclusion for the event-based computation of $\ell/\gamma\beta$ and for the approximation choosing $\langle \ell_{\rm outer}/\gamma\beta \rangle_{\rm eff} = 7\,$m (see text for details). For the direct production we choose the cross section Drell-Yan stau pair production, while the cross section for 1-step decay corresponds to (degenerate) squark production with $m_{\tilde{q}} = m_{\tilde{g}}$.

[2] F. Ambrogi, S. Kraml, S. Kulkarni, U. Laa, A. Lessa, V. Magerl, J. Sonneveld, M. Traub, and W. Waltenberger, *SModelS v1.1 user manual: Improving simplified model constraints with efficiency maps*. Comput. Phys. Commun. **227** (2018) 72–98, arXiv:1701.06586 [hep-ph].

[3] L. Edelhäuser, J. Heisig, M. Krämer, L. Oymanns, and J. Sonneveld, *Constraining supersymmetry at the LHC with simplified models for squark production*. JHEP **12** (2014) 022, arXiv:1410.0965 [hep-ph].

[4] L. Edelhäuser, M. Krämer, and J. Sonneveld, *Simplified models for same-spin new physics scenarios*. JHEP **04** (2015) 146, arXiv:1501.03942 [hep-ph].

[5] C. Arina, M. E. C. Catalan, S. Kraml, S. Kulkarni, and U. Laa, *Constraints on sneutrino dark matter from LHC Run 1*. JHEP **05** (2015) 142, arXiv:1503.02960 [hep-ph].

[6] S. Kraml, U. Laa, L. Panizzi, and H. Prager, *Scalar versus fermionic top partner interpretations of $t\bar{t} + E_T^{\rm miss}$ searches at the LHC*. JHEP **11** (2016) 107, arXiv:1607.02050 [hep-ph].

[7] F. Ambrogi, J. Heisig, S. Kraml, S. Kulkarni, U. Laa, A. Lessa, H. Reyes-Gonzalez, and W. Waltenberger, *SModelS v1.2 release note, in preparation*.

[8] J. Heisig, A. Lessa, and L. Quertenmont, *Simplified Models for Exotic BSM Searches*. JHEP **12** (2015) 087, arXiv:1509.00473 [hep-ph].

[9] **CMS** Collaboration, V. Khachatryan *et al.*, *Search for heavy stable charged particles with* 12.9 fb^{-1} *of 2016 data*, Tech. Rep. CMS-PAS-EXO-16-036, 2016. http://cds.cern.ch/record/2205281.

[10] **CMS** Collaboration, V. Khachatryan *et al.*, *Constraints on the pMSSM, AMSB model and on other models from the search for long-lived charged particles in proton-proton collisions at sqrt(s) = 8 TeV*. Eur. Phys. J. **C75** (2015) no. 7, 325, arXiv:1502.02522 [hep-ex].

[11] **CMS** Collaboration, S. Chatrchyan *et al.*, *Searches for long-lived charged particles in pp collisions at $\sqrt{s}$=7 and 8 TeV*. JHEP **07** (2013) 122, arXiv:1305.0491 [hep-ex].

[12] **Particle Data Group** Collaboration, K. A. Olive *et al.*, *Review of Particle Physics*. Chin. Phys. **C38** (2014) 090001.

[13] A. Ilnicka, M. Krawczyk, and T. Robens, *Inert Doublet Model in light of LHC Run I and astrophysical data*. Phys. Rev. **D93** (2016) no. 5, 055026, arXiv:1508.01671 [hep-ph].

[14] A. Belyaev, G. Cacciapaglia, I. P. Ivanov, F. Rojas-Abatte, and M. Thomas, *Anatomy of the Inert Two Higgs Doublet Model in the light of the LHC and non-LHC Dark Matter Searches*. Phys. Rev. **D97** (2018) no. 3, 035011, arXiv:1612.00511 [hep-ph].

[15] B. Eiteneuer, A. Goudelis, and J. Heisig, *The inert doublet model in the light of Fermi-LAT gamma-ray data: a global fit analysis*. Eur. Phys. J. **C77** (2017) no. 9, 624, arXiv:1705.01458 [hep-ph].

[16] A. Pierce and J. Thaler, *Natural Dark Matter from an Unnatural Higgs Boson and New Colored Particles at the TeV Scale*. JHEP **0708** (2007) 026, arXiv:hep-ph/0703056 [HEP-PH].

[17] Q.-H. Cao, E. Ma, and G. Rajasekaran, *Observing the Dark Scalar Doublet and its Impact on the Standard-Model Higgs Boson at Colliders*. Phys. Rev. D **76** (2007) 095011, arXiv:0708.2939 [hep-ph].

[18] E. Dolle, X. Miao, S. Su, and B. Thomas, *Dilepton Signals in the Inert Doublet Model*. Phys. Rev. D **81** (2010) 035003, arXiv:0909.3094 [hep-ph].

[19] X. Miao, S. Su, and B. Thomas, *Trilepton Signals in the Inert Doublet Model*. Phys. Rev. D **82** (2010) 035009, arXiv:1005.0090 [hep-ph].

[20] M. Gustafsson, S. Rydbeck, L. Lopez-Honorez, and E. Lundstrom, *Status of the Inert Doublet Model and the Role of multileptons at the LHC*. Phys.Rev. **D86** (2012) 075019, arXiv:1206.6316 [hep-ph].

[21] G. Belanger, B. Dumont, A. Goudelis, B. Herrmann, S. Kraml, and D. Sengupta, *Dilepton constraints in the Inert Doublet Model from Run 1 of the LHC*. Phys. Rev. **D91** (2015) no. 11, 115011, arXiv:1503.07367 [hep-ph].

[22] **ATLAS** Collaboration, G. Aad *et al.*, *Search for direct production of charginos, neutralinos and*

sleptons in final states with two leptons and missing transverse momentum in pp collisions at $\sqrt{s} = 8$ TeV with the ATLAS detector. JHEP **05** (2014) 071, arXiv:1403.5294 [hep-ex].

[23] A. Goudelis, B. Herrmann, and O. Stål, *Dark matter in the Inert Doublet Model after the discovery of a Higgs-like boson at the LHC*. JHEP **09** (2013) 106, arXiv:1303.3010 [hep-ph].

[24] **ATLAS** Collaboration, M. Aaboud *et al.*, *Search for electroweak production of supersymmetric states in scenarios with compressed mass spectra at $\sqrt{s} = 13$ TeV with the ATLAS detector*. Phys. Rev. **D97** (2018) no. 5, 052010, arXiv:1712.08119 [hep-ex].

[25] **ATLAS** Collaboration, M. Aaboud *et al.*, *Search for electroweak production of supersymmetric particles in final states with two or three leptons at $\sqrt{s} = 13$ TeV with the ATLAS detector*. arXiv:1803.02762 [hep-ex].

[26] T. Hambye, F.-S. Ling, L. Lopez Honorez, and J. Rocher, *Scalar Multiplet Dark Matter*. JHEP **0907** (2009) 090, arXiv:0903.4010 [hep-ph].

[27] **Planck** Collaboration, P. A. R. Ade *et al.*, *Planck 2015 results. XIII. Cosmological parameters*. Astron. Astrophys. **594** (2016) A13, arXiv:1502.01589 [astro-ph.CO].

[28] G. Belanger, F. Boudjema, A. Pukhov, and A. Semenov, *micrOMEGAs4.1: two dark matter candidates*. Comput. Phys. Commun. **192** (2015) 322–329, arXiv:1407.6129 [hep-ph].

[29] **ATLAS** Collaboration, G. Aad *et al.*, *Constraints on new phenomena via Higgs boson couplings and invisible decays with the ATLAS detector*. JHEP **11** (2015) 206, arXiv:1509.00672 [hep-ex].

[30] **Gfitter Group** Collaboration, M. Baak, J. Cuth, J. Haller, A. Hoecker, R. Kogler, K. Mönig, M. Schott, and J. Stelzer, *The global electroweak fit at NNLO and prospects for the LHC and ILC*. Eur. Phys. J. **C74** (2014) 3046, arXiv:1407.3792 [hep-ph].

[31] D. Eriksson, J. Rathsman, and O. Stal, *2HDMC: Two-Higgs-Doublet Model Calculator Physics and Manual*. Comput. Phys. Commun. **181** (2010) 189–205, arXiv:0902.0851 [hep-ph].

[32] E. Lundström, M. Gustafsson, and J. Edsjö, *The Inert Doublet Model and LEP II Limits*. Phys. Rev. D **79** (2009) 035013, arXiv:0810.3924 [hep-ph].

[33] **DES, Fermi-LAT** Collaboration, A. Albert *et al.*, *Searching for Dark Matter Annihilation in Recently Discovered Milky Way Satellites with Fermi-LAT*. arXiv:1611.03184 [astro-ph.HE].

[34] **XENON** Collaboration, E. Aprile *et al.*, *Dark Matter Search Results from a One Tonne× Year Exposure of XENON1T*. arXiv:1805.12562 [astro-ph.CO].

[35] F. Feroz, M. P. Hobson, and M. Bridges, *MultiNest: an efficient and robust Bayesian inference tool for cosmology and particle physics*. Mon. Not. Roy. Astron. Soc. **398** (2009) 1601–1614, arXiv:0809.3437 [astro-ph].

[36] F. Feroz, M. P. Hobson, E. Cameron, and A. N. Pettitt, *Importance Nested Sampling and the MultiNest Algorithm*. arXiv:1306.2144 [astro-ph.IM].

[37] J. Alwall, R. Frederix, S. Frixione, V. Hirschi, F. Maltoni, O. Mattelaer, H. S. Shao, T. Stelzer, P. Torrielli, and M. Zaro, *The automated computation of tree-level and next-to-leading order differential cross sections, and their matching to parton shower simulations*. JHEP **07** (2014) 079, arXiv:1405.0301 [hep-ph].

[38] P. Fayet, "Experimental consequences of supersymmetry," in *Proceedings of the XVIth Rencontre de Moriond*, J. Tran Thanh Van, ed., vol. 1, pp. 347–367. Editions Frontieres, 1981.

[39] H. Pagels and J. R. Primack, *Supersymmetry, Cosmology and New TeV Physics*. Phys. Rev. Lett. **48** (1982) 223.

[40] S. Weinberg, *Cosmological Constraints on the Scale of Supersymmetry Breaking*. Phys. Rev. Lett. **48** (1982) 1303.

[41] J. R. Ellis, J. E. Kim, and D. V. Nanopoulos, *Cosmological Gravitino Regeneration and Decay*. Phys. Lett. **B145** (1984) 181.

[42] I. V. Falomkin, G. B. Pontecorvo, M. G. Sapozhnikov, M. Y. Khlopov, F. Balestra, and G. Piragino, *Low-energy $\bar{p}\,^4He$ Annihilation And Problems Of The Modern Cosmology, GUT And SUSY Models*. Nuovo Cim. **A79** (1984) 193–204. [Yad. Fiz. **39** (1984), 990].

[43] J. R. Ellis, D. V. Nanopoulos, and S. Sarkar, *The Cosmology of Decaying Gravitinos*. Nucl. Phys. **B259** (1985) 175.

[44] T. Moroi, H. Murayama, and M. Yamaguchi, *Cosmological constraints on the light stable gravitino*. Phys. Lett. **B303** (1993) 289–294.

[45] M. Bolz, W. Buchmuller, and M. Plumacher, *Baryon asymmetry and dark matter*. Phys. Lett. **B443** (1998) 209–213, arXiv:hep-ph/9809381 [hep-ph].

[46] M. Bolz, A. Brandenburg, and W. Buchmuller, *Thermal production of gravitinos*. Nucl. Phys. **B606** (2001) 518–544, arXiv:hep-ph/0012052 [hep-ph]. [Erratum: Nucl. Phys.B790,336(2008)].

[47] J. Pradler and F. D. Steffen, *Constraints on the Reheating Temperature in Gravitino Dark Matter Scenarios*. Phys. Lett. **B648** (2007) 224–235, arXiv:hep-ph/0612291 [hep-ph].

[48] J. Heisig, J. Kersten, B. Panes, and T. Robens, *A survey for low stau yields in the MSSM*. JHEP **04** (2014) 053, arXiv:1310.2825 [hep-ph].

[49] J. Heisig, *Gravitino LSP and leptogenesis after the first LHC results*. JCAP **1404** (2014) 023, arXiv:1310.6352 [hep-ph].

[50] A. Djouadi, J.-L. Kneur, and G. Moultaka, *SuSpect: A Fortran code for the supersymmetric and Higgs particle spectrum in the MSSM*. Comput. Phys. Commun. **176** (2007) 426–455, arXiv:hep-ph/0211331 [hep-ph].

[51] S. Heinemeyer, W. Hollik, and G. Weiglein, *FeynHiggs: A Program for the calculation of the masses of the neutral CP even Higgs bosons in the MSSM*. Comput. Phys. Commun. **124** (2000) 76–89, arXiv:hep-ph/9812320 [hep-ph].

[52] G. Degrassi, S. Heinemeyer, W. Hollik, P. Slavich, and G. Weiglein, *Towards high precision predictions for the MSSM Higgs sector*. Eur. Phys. J. **C28** (2003) 133–143, arXiv:hep-ph/0212020 [hep-ph].

[53] A. Djouadi, M. M. Muhlleitner, and M. Spira, *Decays of supersymmetric particles: The Program SUSY-HIT (SUspect-SdecaY-Hdecay-InTerface)*. Acta Phys. Polon. **B38** (2007) 635–644, arXiv:hep-ph/0609292 [hep-ph].

[54] S. Kraml and D. T. Nhung, *Three-body decays of sleptons in models with non-universal Higgs masses*. JHEP **02** (2008) 061, arXiv:0712.1986 [hep-ph].

[55] G. Belanger, F. Boudjema, A. Pukhov, and A. Semenov, *Dark matter direct detection rate in a generic model with micrOMEGAs 2.2*. Comput. Phys. Commun. **180** (2009) 747–767, arXiv:0803.2360 [hep-ph].

[56] P. Bechtle, O. Brein, S. Heinemeyer, G. Weiglein, and K. E. Williams, *HiggsBounds 2.0.0:*

Confronting Neutral and Charged Higgs Sector Predictions with Exclusion Bounds from LEP and the Tevatron. Comput. Phys. Commun. **182** (2011) 2605–2631, arXiv:1102.1898 [hep-ph].

[57] **CDF, D0** Collaboration, T. E. W. Group, *2012 Update of the Combination of CDF and D0 Results for the Mass of the W Boson*. arXiv:1204.0042 [hep-ex].

[58] P. Bechtle, S. Heinemeyer, O. Stal, T. Stefaniak, G. Weiglein, and L. Zeune, *MSSM Interpretations of the LHC Discovery: Light or Heavy Higgs?* Eur. Phys. J. **C73** (2013) no. 4, 2354, arXiv:1211.1955 [hep-ph].

[59] S. Heinemeyer, W. Hollik, D. Stockinger, A. M. Weber, and G. Weiglein, *Precise prediction for M(W) in the MSSM*. JHEP **08** (2006) 052, arXiv:hep-ph/0604147 [hep-ph].

[60] T. Kitahara and T. Yoshinaga, *Stau with Large Mass Difference and Enhancement of the Higgs to Diphoton Decay Rate in the MSSM*. JHEP **05** (2013) 035, arXiv:1303.0461 [hep-ph].

[61] J. M. Frere, D. R. T. Jones, and S. Raby, *Fermion Masses and Induction of the Weak Scale by Supergravity*. Nucl. Phys. **B222** (1983) 11–19.

[62] L. Alvarez-Gaume, J. Polchinski, and M. B. Wise, *Minimal Low-Energy Supergravity*. Nucl. Phys. **B221** (1983) 495.

[63] M. Claudson, L. J. Hall, and I. Hinchliffe, *Low-Energy Supergravity: False Vacua and Vacuous Predictions*. Nucl. Phys. **B228** (1983) 501–528.

[64] C. Kounnas, A. B. Lahanas, D. V. Nanopoulos, and M. Quiros, *Low-Energy Behavior of Realistic Locally Supersymmetric Grand Unified Theories*. Nucl. Phys. **B236** (1984) 438–466.

[65] J. P. Derendinger and C. A. Savoy, *Quantum Effects and SU(2) x U(1) Breaking in Supergravity Gauge Theories*. Nucl. Phys. **B237** (1984) 307–328.

[66] **HFLAV** Collaboration, Y. Amhis *et al.*, *Averages of b-hadron, c-hadron, and τ-lepton properties as of summer 2016*. Eur. Phys. J. **C77** (2017) no. 12, 895, arXiv:1612.07233 [hep-ex].

[67] **LHCb** Collaboration, R. Aaij *et al.*, *Measurement of the $B_s^0 \to \mu^+\mu^-$ branching fraction and effective lifetime and search for $B^0 \to \mu^+\mu^-$ decays*. Phys. Rev. Lett. **118** (2017) no. 19, 191801, arXiv:1703.05747 [hep-ex].

[68] **CMS** Collaboration, A. M. Sirunyan *et al.*, *Search for additional neutral MSSM Higgs bosons in the $\tau\tau$ final state in proton-proton collisions at $\sqrt{s} = 13$ TeV*. arXiv:1803.06553 [hep-ex].

[69] K. Jedamzik, *Bounds on long-lived charged massive particles from Big Bang nucleosynthesis*. JCAP **0803** (2008) 008, arXiv:0710.5153 [hep-ph].

[70] K. Jedamzik, *Big bang nucleosynthesis constraints on hadronically and electromagnetically decaying relic neutral particles*. Phys. Rev. **D74** (2006) 103509, arXiv:hep-ph/0604251 [hep-ph].

[71] P. Sreekumar, F. W. Stecker, and S. C. Kappadath, *The extragalactic diffuse gamma-ray emission*. AIP Conf. Proc. **410** (1997) no. 1, 344, arXiv:astro-ph/9709258 [astro-ph].

[72] G. D. Kribs and I. Z. Rothstein, *Bounds on longlived relics from diffuse gamma-ray observations*. Phys. Rev. **D55** (1997) 4435–4449, arXiv:hep-ph/9610468 [hep-ph]. [Erratum: Phys. Rev.D56,1822(1997)].

[73] K. Hagiwara, K. Mawatari, and Y. Takaesu, *HELAS and MadGraph with spin-3/2 particles*. Eur. Phys. J. **C71** (2011) 1529, arXiv:1010.4255 [hep-ph].

[74] J. Alwall, P. Demin, S. de Visscher, R. Frederix, M. Herquet, F. Maltoni, T. Plehn, D. L. Rainwater, and T. Stelzer, *MadGraph/MadEvent v4: The New Web Generation*. JHEP **09** (2007) 028, arXiv:0706.2334 [hep-ph].

[75] G. Brooijmans *et al.*, "Les Houches 2017: Physics at TeV Colliders New Physics Working Group Report," in *10th Les Houches Workshop on Physics at TeV Colliders (PhysTeV 2017) Les Houches, France, June 5-23, 2017*. 2018. arXiv:1803.10379 [hep-ph]. http://inspirehep.net/record/1664565/files/1803.10379.pdf.